The Development of a Motion-Tracking System to Assess the Recovery Level for Stroke Survivors

Thanh-Trung Nguyen, Quang-Duy Nguyen, Minh-Quang Ha, Xuan-Tung Hoang

School of Mechanical Engineering, Hanoi University of Science and Technology, No. 1 Dai Co Viet, 100000 Hanoi, Vietnam; trung.nguyenthanh@hust.edu.vn; duy.nq194987@sis.hust.edu.vn; quang.hm195147@sis.hust.edu.vn; tung.hx195223@sis.hust.edu.vn

Tam-Ngoc Bui

Shibaura Institute of Technology, 307 Fukasaku, 337-8570 Saitama, Japan; tambn@shibaura-it.ac.jp

Duc-Luu Tien

National Institute of Patent and Technology Exploitation, 113 Tran Duy Hung street, 10072 Hanoi, Vietnam; ltduc@most.gov.vn

Abstract: Stroke is a widespread and perilous condition globally, necessitating effective rehabilitation assessment methods. Presently, clinicians rely on manual observation or costly equipment like motion capture systems to evaluate stroke patients' recovery progress. This study introduces a streamlined measurement system designed for assessing lower limb function recovery in stroke patients. The system employs wearable IMU (Inertial Measurement Unit) sensor modules strategically placed on the lower limbs to capture joint angles. An algorithm processes sensor data to calculate precise joint angles. To counteract environmental interference affecting IMU sensors, a Kalman filter is implemented to minimize errors, providing real-time adjustments for sensor accuracy. Experimental validation, using exercises and criteria from the FUGL-MEYER Assessment, a widely adopted method for evaluating stroke patients' physical performance, was conducted to compare the proposed system with the VICON motion capture system. Results demonstrated close alignment between the two systems, affirming the proposed system's reliability, applicability, and practicality for real-life medical evaluations. Importantly, the proposed system offers a cost-effective and portable alternative for measuring joint angles, maintaining effectiveness and precision. In summary, this system offers a straightforward design, easy installation, and affordable hardware, making it a viable and practical solution for evaluating lower limb rehabilitation in stroke patients.

Keywords: IMU sensors; Kalman filter; Fugl-Meyer Assessment; lowerlimb; Vicon Motion Capture System

1 Introduction

Stroke is a medical condition that occurs when the blood supply to a part of the brain is blocked, interrupted, or reduced, causing deprivation of oxygen to brain cells. The World Health Organization (WHO) reported that stroke is the second leading cause of death and the third leading cause of disability [1]. According to the World Stroke Organization (WSO), there are over 12.2 million new strokes each year, with a survival rate of only 46.7% [2]. In Vietnam, the stroke incidence rate is estimated to be 161 per 100,000 people per year [3], and according to WHO in 2020, stroke deaths in Vietnam reached 159,032 or 23.2% of total deaths that year [4]. Patients who experienced a stroke and survived often face severe consequences and challenges, such as limb paralysis, which drastically change their way of living.

It is reported that between 70-85% of stroke survivors experience hemiplegia (paralysis of one side of the body), which often affects the lower body [5]. To help these patients regain their motor functions and return to their formal daily life, physical rehabilitation therapies were developed, widely adopted, and progressively proven to be effective in assisting patients on their journey to recovery.

A critical phase in any therapy is the assessment of the patient's progress. Progress evaluation is often based on a certain scale like NIHSS, mRS, or BI, which helps doctors assess the patient's recovery on various aspects using different methods and exercises. For physical rehabilitation, especially lower limb, the Fugl-Meyer Assessment (FMA) is found to be among the most objective, simplest, and effective scale that is commonly used by physicians. The FMA method was designed to evaluate the upper and lower limb motor recovery of stroke patients through simple, visually guided exercises with predefined ratings, which help make the evaluation process easy for both the doctor and the patient [6]. However, traditional FMA depends heavily on the doctor's subjective observations, which sometimes could be unreliable and incorrect [7]. Moreover, the prospect of storing the patients' motion data for reviewing later is still rather limited. This study aims to develop a system that can counter these drawbacks, reducing the need for manual monitoring and providing the ability to log the patient's data. To accomplish these tasks, the patient's joint angles, the hip, knee, and ankle angles, are needed. With that goal in mind, along with wearability and portability, the Inertial Measurement Unit (IMU) sensor is a great candidate for this research.

In fact, numerous studies have used IMU sensors to measure body joint angles for different applications [8] [9], most of which reported their accuracy and performance to be well acceptable. The sensors are considered small, versatile, and reliable systems suitable for wearables that do not impede movements [10] [11]. This allows them to be effectively integrated into the assessment process, helping healthcare professionals to evaluate the patient's progress more objectively and accurately, without being at the expense of their comfort. The IMU sensor in this research is the BNO055 from Adafruit Industries, which is based on the BNO055 9-DoF sensor from Bosch SensorTec. It is a popular sensor module for its affordable price, and compact design with multiple functionalities, especially the integrated Kalman filter which boosts the stability and accuracy of the output data [12].

To verify the integration of BNO055 into rehabilitation evaluation, as well as its precision and performance in the process, the module's collected data was compared to those obtained from the current "gold standard" for evaluating lower limb kinematics, which is VICON, a three-dimensional motion analysis (3DMA)system [13]. VICON used multiple cameras placed around the room to fully capture all ranges of motion of the subject in three dimensions. It was used with Vicon Nexus and Plug-in Gait lower body model for the joint angles of the lower limbs [14].

After the system was successfully built, experiments were conducted involving using it simultaneously with the VICON system while doing exercises from the FMA method, which are Hip Flexion, Knee Flexion, and Ankle Dorsiflexion. The BNO055s were strapped onto the abdomen, thigh, body shank, and foot. Data from the sensors were transmitted to the Arduino Mega 2560, a microcontroller board, via I2C protocol, which calculated the joint angles by putting the data through an algorithm. The results were then sent to a computer via USB connection to be displayed and stored.

The rest of the paper is organized as follows. The theoretical bases of this research are provided in Section 2, which includes details on the FMA method, the Kalman filter, and the BNO055 sensor module along with its calibration. The proposed method and system design are presented in Section 3. Conducted experiments are demonstrated in Section 4, while comparison with VICON data and results discussions are given in Section 5. Finally, conclusions and future work are stated in conclusions.

2 Theoretical Foundations

2.1 The Basis of Functional Recovery Assessment Method

The assessment of a stroke patient's recovery is often combined with scales to create a comprehensive picture of the patient's health status and recovery level. There are several commonly used scales to assess functional recovery, such as the National Institutes of Health Stroke Scale (NIHSS), modified Rankin Scale (mRS), Barthel Index (BI), Fugl-Meyer Assessment (FMA), Canadian Neurological Scale (CNS), and more. The NIHSS is a highly accurate tool to evaluate the severity of stroke via neurological functions in stroke survivors including level of consciousness, visual fields, movement of facial muscles, and movement of upper and lower extremity [15]. Another simple tool used in assessing neurological status of stroke patients is the CNS, which evaluates 10 clinical domains including mentation and motor function in the acute phase of stroke [16]. In addition to these recovery evaluation scales, the mRS is a 7-point hierarchical scale applied in functional independence measurement. The broad concentration provided by mRS potentially goes beyond the basic scale measuring Activities of Daily Living (ADLs), upon which the BI operates to assess poststroke outcomes in stroke trials [17].

The Fugl-Meyer Assessment (FMA) is also one of the most commonly used tools to support the evaluation of functional recovery for stroke patients. The FMA comprises a set of performance-based impairment indexes that evaluate motor functioning, sensation, balance, joint range of motion and joint pain in stroke survivors [18]. The FMA possesses some advantages compared to other recovery evaluation scales such as NIHSS, mRS and BI. First, FMA is more stroke-specific and reflects the natural history of motor recovery after stroke, while NIHSS, mRS and BI can be used for other neurological conditions due to their generality [18] Secondly, FMA covers more domains (5 domains in total) than NIHSS, mRS and BI, with the former only focusing on neurological deficits [15] and the two latters only assessing functional dependence [17]. Thirdly, FMA is more objective than mRS, which are mainly based on subjective ratings through interviews with patients that also leads to inter-observer variability – the main drawback of mRS [17]. Finally, the fourth benefit of FMA comes from its sensitivity and responsiveness to minor improvements or deteriorations in stroke recovery [18], which result in better reliability compared to NIHSS, mRS and BI.

Given the aforementioned benefits, FMA was selected as the standard in this study to measure the extent of functional recovery among stroke patients. Even though it has shown advantages over alternative assessment scales, the traditional scoring technique still mostly relies on medical staff members' direct observation [19]. As a result, this may lead to less reliable results and make it more difficult to gather and save patient movement data for later analysis. In order to address these

shortcomings, numerous studies have incorporated Inertial Measurement Units (IMU) into motion capture apparatuses to obtain more precise kinematic data [20] [21]. With the help of this integration, medical professionals can now evaluate stroke patients' progress with greater objectivity and accuracy, and they can now provide targeted treatment plans with specific information. Therefore, the primary goal of this research is to create a motion data gathering system that is integrated with IMU sensors and assess how the model might be used to measure patients' functional recovery, using FMA as the assessment tool.

The upper extremity has 33 items on the FMA scale, whereas the lower extremity has 17 items. Every item is rated on a 3-point rating scale: with 0, 1 and 2 respectively represents an inability to perform, a partial performance, and full performance. The possible maximum score for upper extremity and lower extremity are 66 and 34 points respectively [22]. Nonetheless, the primary function of FMA in this study is to serve as a scale to evaluate the developed IMU-integrated system's potential use in gathering motion data from stroke survivors. For that reason, and in order to streamline and expedite the evaluation process during the system's initial development phase, the article only focuses on the FMA evaluation of the lower extremity's range of motion. The selected section consists of 3 exercises: Hip Flexion (beyond 90^o), Knee Flexion (beyond 90^o) and Ankle Dorsiflexion (beyond 5^o) [19] that assess movement range of hip, knee and ankle joints of lower limbs. These chosen movements are executed within the sagittal plane, with the required range of motion of lower limb's joints that when combined can allow patients to perform Walking exercise in the later stage of the functional recovery process.

2.2 Kalman Filter

The Kalman filter algorithm is a method for estimating the state of a dynamic system based on measurements and the system's predictive model [23]. The algorithm was developed by Rudolf E. Kalman in 1960 and has become one of the most-used tools in the field of signal processing and automatic control.

During signal measurement, sensors are very sensitive to measurement noise and external noise, which causes errors in the measured values. The Kalman filter is an effective filter in solving unobservable noise. It is designed to handle state estimation problems in noisy environments. The Kalman Filter Algorithm provides an efficient method for updating and predicting the system's state based on measurements and dynamic models. The algorithm operates in two main steps: prediction and update.

(1) Prediction: In this step, the algorithm uses the system's dynamic model to predict the next state. This prediction is often performed through a transition matrix and a control vector.

(2) Update: In this step, the algorithm uses new measurement information to update the estimated state of the system. This update assumes that the measurement information has some noise, and it will compute an optimal estimate of the state based on both the previous prediction and the current state.

The model of the algorithm can be described as follow:

$$\begin{cases} \vec{x_t} = F.\vec{x_{t-1}} + B.\vec{u_{t-1}} + \vec{\omega}_{t-1} \\ \vec{z_t} = H.\vec{x_t} + \vec{v_t} \end{cases} \quad (1)$$

With $\vec{\omega}_t \sim N(0,Q_t)$ being the process noise and $\vec{v_t} \sim N(0,R_t)$ being the measurement noise obeying the Gaussian distribution. Q_t and R_t are the corresponding noise matrices for the process noise and measurement noise. The state would be predicted based on the previous state using the state transition matrix F, where $\vec{u_t}$ is the control vector, B is the control matrix. At this point, we have the prediction equation from the output of the filter at the previous step and the transition matrix:

$$\vec{x}_{t|t-1} = F.\vec{x}_{t|t-1} \quad (2)$$

With covariance prediction:

$$P_{t|t-1} = F_t.P_{t-1|t-1}.F_t^T + Q_t \quad (3)$$

Update the state using the observation matrix $\vec{z}_t$. Matrix H represents the mapping between the state space and the measurement space.

Update the estimated state:

$$\vec{x}_{t|t} = \vec{x}_{t|t-1} + K.(z_t - \vec{x}_{t|t-1}) \quad (4)$$

With Kalman gain:

$$K = P_{t|t-1}.H.(H.P_{t|t-1}.H^T + R)^{-1} \quad (5)$$

Update the error covariance:

$$P_{t|t} = (I - K_t.H).P_{t|t-1} \quad (6)$$

The Kalman Filter algorithm is used in various fields such as automatic control, image processing, positioning, and measurements. It has become an important tool in applications that require tracking and predicting the state of dynamic systems, including the IMU-based motion capture system developed in this research.

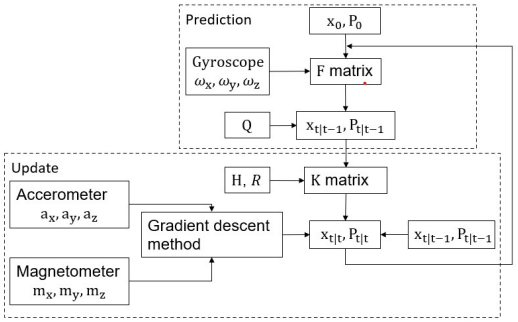

Figure 1
Kalman filter block diagram

2.3 IMU BNO055 Sensor

The BNO055 stands out as a sophisticated Inertial Measurement Unit (IMU) sensor, seamlessly integrating a 3-axis 14-bit accelerometer, a 3-axis 16-bit gyroscope, and a 3-axis magnetometer [12]. The accelerometer detects linear acceleration, including gravity, while the gyroscope tracks angular rotation, and the magnetometer provides a reference to the Earth's magnetic field, allowing the sensor to determine the orientation relative to magnetic north. Overall, this powerful combination of magnetometer, accelerometer and gyroscope data enables the sensor to furnish comprehensive data, including absolute orientation information in the form of Euler angles and quaternions, as well as crucial parameters such as acceleration, angular velocity, and magnetic field data. This paper uses Euler angles outputs, which the sensor detect in the range of -180˚ to 180˚ for pitch values, -90˚ to 90˚ for roll values and 0˚ to 360˚ for yaw values. The collected data is updated at the rate of 100Hz.

Despite the gyroscope's primary role in measuring angular velocity, its long-term reliability is compromised by temperature-induced sensor errors, leading to the accumulation of inaccuracies over extended periods [24]. To counteract this issue, a dynamic mechanism is employed wherein inclination values derived from the accelerometer are used to finely adjust the gyroscope's bias. This adjustment is critical for enhancing the accuracy of angular velocity measurements. Consequently, improving the overall precision of the IMU [24] [25] [26].

However, the accelerometer, while proficient in many respects, has its limitations. Notably, it falls short in detecting rotations around the vertical axis. This deficiency underscores the importance of the magnetometer in the sensor's architecture. Leveraging the magnetometer's high sensitivity to Earth's magnetic field, the BNO055 employs it judiciously to correct the gyroscope's bias specifically for rotations around the vertical axis. This strategic integration ensures

a more comprehensive and accurate orientation estimation, compensating for the accelerometer's inherent limitations. To further refine the data output and mitigate potential inaccuracies arising from sensor noise and uncertainties, a Kalman filter has been seamlessly incorporated into the BNO055's processing pipeline. The implemented Kalman filter compensates for errors and noise by continuously estimating the true orientation based on the fusion of accelerometer, gyroscope, and magnetometer data. It dynamically adjusts the weighting of each sensor's contribution based on their respective uncertainties to provide accurate orientation measurements. This results in a more robust and precise estimation of Euler angles and quaternions. The Kalman filter acts as a crucial component in enhancing the overall performance of the BNO055, especially in dynamic and challenging environments where accurate orientation data is paramount [27]. In essence, the BNO055's design represents a holistic approach to IMU sensing, addressing the intricacies of each sensor component and seamlessly integrating them into a coherent system. Through the dynamic interplay of the accelerometer, gyroscope, and magnetometer, complemented by the intelligent application of a Kalman filter, the BNO055 stands as a reliable solution for applications requiring accurate and stable orientation data over time.

2.4 Sensors Calibration

Even with the Kalman filter's ability to fuse sensors, the calibration procedure that comes before IMU operation is still necessary to guarantee measurement accuracy and dependability. Firstly, even though the Kalman filter excels at mitigating the mistakes of uncertain sensors, it might not be able to completely compensate for systembased errors of IMUs including biases, misalignments, and scaling factors. Thus, in order to produce more dependable results, the calibration procedure must locate and fix those systematic mistakes. Second, IMU sensor calibration lays the groundwork for the Kalman filter estimation process, which needs precise baseline data in order to interpret sensor data as best it can. Additionally, the process of calibration can improve the overall performance of the Kalman filter by improving the IMU's ability to adapt to changes in the environment, accounting for non-Gaussian errors brought on by outside disturbances like magnetic interference, and identifying and compensating for crossaxis effects that have been observed in some IMU sensors. In conclusion, because of the complementing properties of the calibration steps—which help handle uncertainties that the Kalman filter does not fully address—the combination of calibration and Kalman filter paves the way for the highest level of operational accuracy and performance in IMU-based systems.

An IMU sensor's calibration procedures can differ based on the model of the sensor and the manufacturer's instructions, but a typical method usually entails a few essential phases that are covered in-depth in this paragraph. It is necessary to set up a controlled environment with consistent temperature, low vibration, and magnetic impedance before the calibration procedure can start. The IMU would

then be placed on a level surface by the calibration specialist in the initial orientation, which may be either upright or flat. To provide accurate calibration data, carefully follow these instructions after completing pre-calibration setups [12]:

- *Gyroscope bias calibration*: The IMU sensor, specifically BNO055 in this study, should be held standing in any stationary position to estimate the gyroscope biases. This helps enhance the accuracy of angular velocity measurements.
- *Accelerometer calibration*: The BNO055 must be placed at rest in 6 standing positions [12] that shown in Figure 2. This helps estimate accelerometer biases and scale factors as well as compensate for the influence of cross-axis effects.
- *Magnetometer calibration*: The sensor should be held parallel to the ground and moved along the pattern illustrated in Figure 3. This allows correction of errors caused by magnetic disturbances.

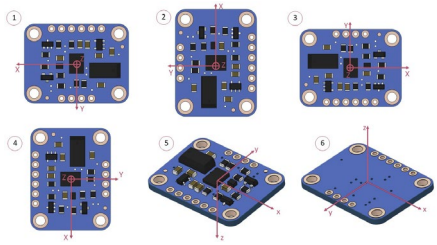

Figure 2
Six stable positions for Accelerometer Calibration

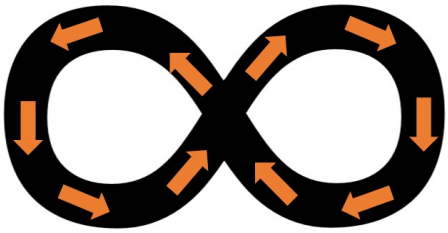

Figure 3
Magnetometer Calibration

3 Proposed Method For System Development

3.1 Measurement Principle

The system consists of 4 IMU sensors placed at the abdomen, thigh, shank, and foot positions to measure the motion of the hip joint, knee joint, and ankle joint. Each IMU sensor will measure Euler angle values based on accelerometer, gyroscope, and magnetometer for calculations. For the purpose of measuring the movements of FMA, including Hip Flexion, Knee Flexion, and Ankle Dorsiflexion, which are movements in the 2D plane, this study only needs to use the pitch angle of each IMU. The description of the Hip, Knee, and Ankle angles is shown in the Figure 4. The angles are calculated by:

$$\begin{aligned} Hip_{angle} &= |\theta_{IMU_1}| - |\theta_{IMU_2}| \\ Knee_{angle} &= |\theta_{IMU_3}| - |\theta_{IMU_2}| \\ Ankle_{angle} &= |\theta_{IMU_4}| - |\theta_{IMU_3}| - 90 \end{aligned} \tag{7}$$

With ϕ_{IMU_i}, θ_{IMU_i}, ψ_{IMU_i} respectively being the roll, pitch, yaw angle of the IMU number i.

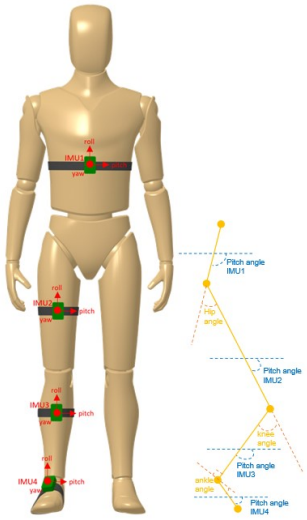

Figure 4
Measurement principle

Figure 5
Overall structure of the system

3.2 Wiring Diagram

As exhibited in Figure 6, the Arduino Mega 2560 is used as the central control unit. It facilitates signal reception from the entire Inertial Measurement Unit (IMU) array through the I2C communication standard. By default, each IMU is assigned one of two unique IDs: 0x78 and 0x79. To enable a single controller to read data from all four IMUs, an TCA9548a expansion module is employed. This module aids in the identification of each sensor, allowing the Arduino to accurately discern the received signals from the IMUs [12].

3.3 Hardware Design

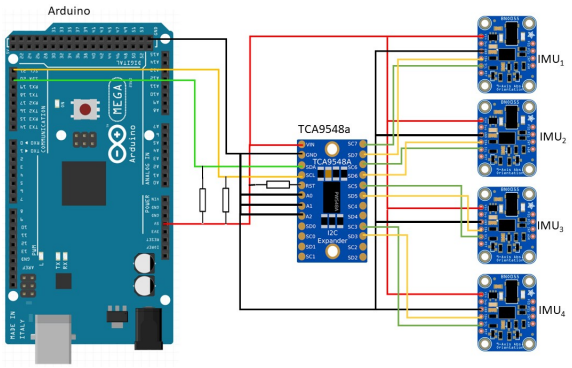

Figure 6
Wiring diagram of the system

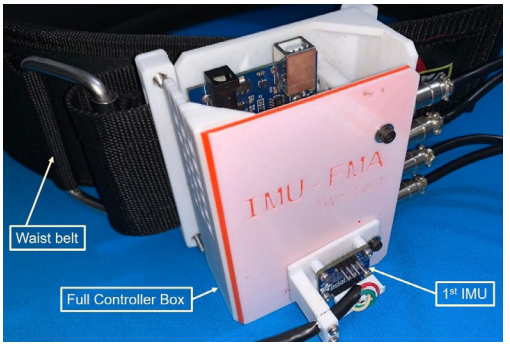

Figure 7
Full Controller Box fastened to waist belt, with the first IMU attached to the lid

As being illustrated in Figure 5, the overall structure of the system consists of two main clusters: the Controller Box (1) and the IMU Box (2). The Controller Box is the location housing the central control board, Arduino Mega 2560, responsible for receiving Euler angle data from IMU sensors to process, calculate joint angles of the Hip, Knee, Ankle, and transmit the computed results to the display for the user. The Controller Box is positioned at the abdomen on the user's body, secured by a waist belt to minimize displacement during movement. On the lid of the Controller Box, IMU number 1 is attached to determine the coordinate system's orientation for the entire measurement system (Figure 7).

Meanwhile, the IMU Box is tasked with securely fixing IMU sensors at predefined positions (abdomen, thigh, shin, foot) using flexible joint belts to ensure stable data acquisition during the execution of movements in this research.

Additionally, the IMU boxes are installed flat with each other for the convenience of computing lower limb joint angle data. Signal transmission between the IMU Box and Controller Box is executed through shielded signal cables, ensuring stability and reliability of the collected data. These connections are standardized with GX16-4P jack plugs, facilitating quick and easy installation while maintaining a stable physical connection. Exploded views of IMU Boxand Controller Box are demonstrated in Figures 8, 9.

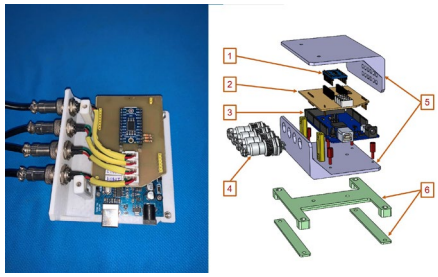

Figure 8
Components of Controller Box: 1) TCA9548A; 2) PCB shield; 3) Arduino Mega2560; 4) GX16-4P jack plug; 5) Controller box cover; 6) Waist belt clamp

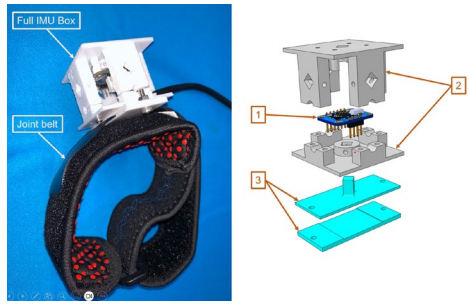

Figure 9
Components of IMU Box: 1) IMU sensor; 2) IMU Box cover; 3) Joint belt clamp

4 Experiment

4.1 Experiment Setup

To test the stability of the equipment and verify the accuracy of the collected data, measurements of the motion data were conducted for three movements within the FMA scale, including Hip Flexion, Knee Flexion, and Ankle Dorsiflexion

simultaneously using both the IMU-based system and Optical Motion Capture (MOCAP). In the initial evaluation phase of the system, experiments were performed on healthy subjects to assess the ability to collect a complete, accurate range of motion for the lower limb joints. If the results are promising, in the subsequent testing phase, the system will be tested in collecting joint angle data on patients recovering from functional rehabilitation.

Each FMA movement was performed by five healthy individuals aged 18-25, with weights ranging from 50-65 kg. First, the necessary parameters of the subjects, including height, weight, ankle width, knee width, and leg length, were measured and carefully recorded. Next, IMU boxes were mounted on segments of the lower limbs of the test subjects (abdomen, thigh, shin, foot), and 14 markers were attached to predetermined positions [11]. All markers were directly applied to the skin at predefined positions (Figure 10a, b) to avoid data discrepancies caused by clothing. Signal cables were neatly wrapped close to the body to prevent hindrance to movement and to obscure the markers of the MOCAP system. The reflective components of the system were covered securely to avoid interfering with the MOCAP measurement signals. After setting up the system on the body, the operator assumed a T-pose at the coordinate origin of the MOCAP system to ensure that the system was accurately configured and ready for the measurement process (Figure 10c)

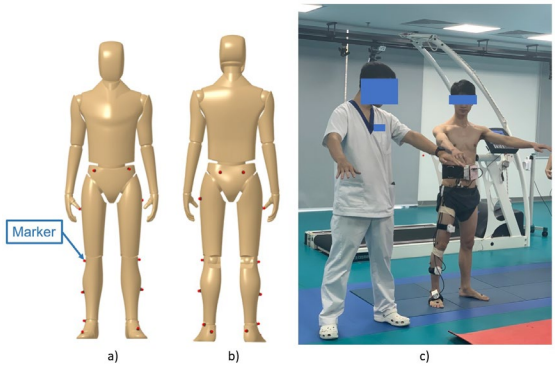

Figure 10
Illustration of marker positions a) Front view; b) Back view;
c) T-pose stance before measurement process

4.2 Experiment Process

After completing the setup phase, the test subjects will sequentially perform three movements: Hip Flexion, Knee Flexion, and Ankle Dorsiflexion, similar to the exercises established on the FMA scale. The exercises selected from the original FMA scale are typically performed in a straight lying or sitting posture. However,

these positions may lead to marker obstruction during measurements. To mitigate this risk, participants in the experiment will execute the movements while standing upright. The prepa ration and execution postures for each exercise are detailed below (Figure 11). The duration for each movement is 1 minute.

- Hip Flexion:
  - Preparation: Stand upright with both feet touching the ground, and slightly shift the measured leg forward.
  - Execution: Lift the hip joint as much as possible towards the upper body while bending the knee.
- Knee Flexion:
  - Preparation: Stand upright, bend one knee so that the thigh is perpendicular to the body, and let the shin hang parallel to the body.
  - Execution: Keep the thigh in place and bend the knee as much as possible.
- Ankle Dorsiflexion:
  - Preparation: Stand on one leg, raise the entire other leg at an angle of approximately $30^{\circ} - 40^{\circ}$ relative to the body, and straighten the raised leg.
  - Execution: Flex the ankle joint as much as possible.

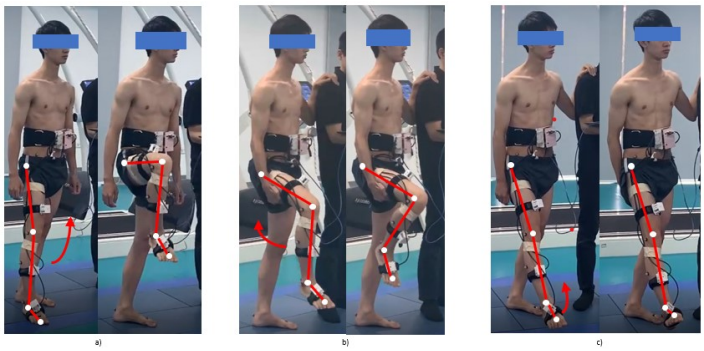

Figure 11
Demonstration of FMA movements: a) Hip Flexion; b) Knee Flexion; c) Ankle Dorsiflexion

5 Result

Figures 12, 13, 14 respectively compare the motion data of Hip, Knee, Ankle joint simultaneously measured on the IMU-integrated system and the MOCAP system. The deviation of data between two systems is calculated using the RMSE formula.

$$RMSE = \sqrt{\frac{\sum_{i=1}^{n}(y_i - \hat{y}_i)^2}{n}} \tag{8}$$

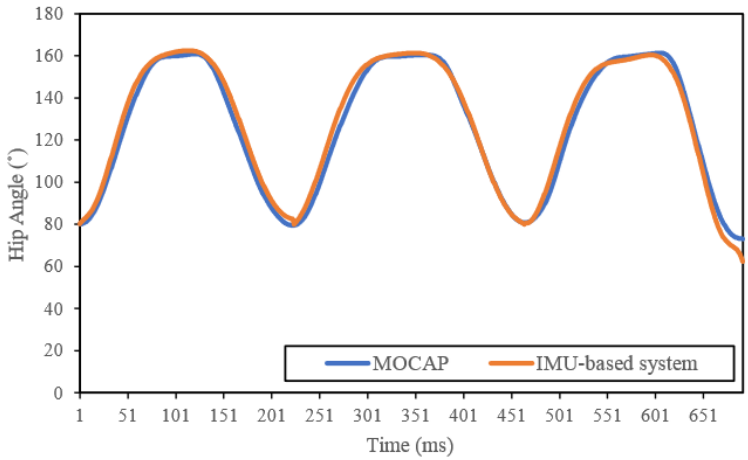

Figure 12
Hip Flexion data comparison

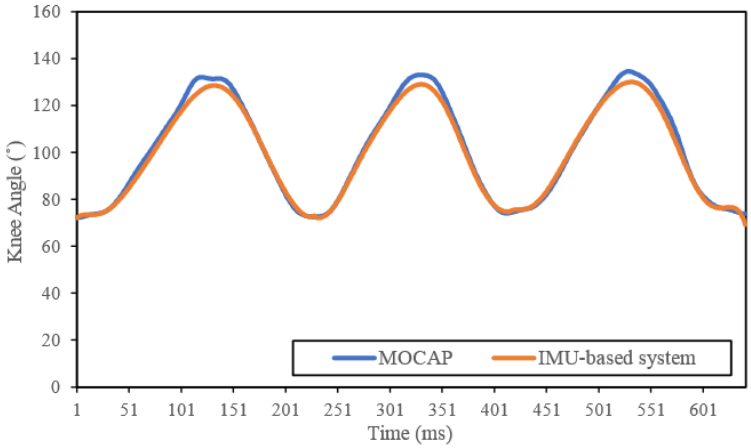

Figure 13
Knee Flexion data comparison

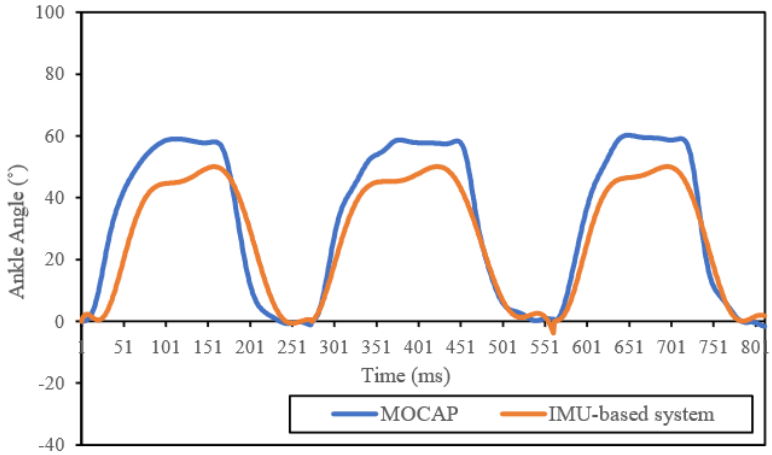

Figure 14
Ankle Dorsiflexion data comparison

The deviation between the data of Hip Flexion and Knee Flexion movements is 3.98˚ and 2.40˚, respectively, while the Ankle Dorsiflexion movement shows a relatively large error of 9.926˚. Therefore, the Knee Flexion data is the most accurate, slightly bigger than the ideal level (ideal error is < 2˚). Although the RMSE error for Hip Flexion is larger than Knee Flexion, it still falls within an acceptable range (< 5˚). However, the Ankle Dorsiflexion data exhibits a considerable error exceeding the acceptable threshold (> 5˚) [28]. The significant error in Ankle Dorsiflexion data may be attributed to the placement of IMU box number 4 on the instep of the performer's foot. Due to the uneven slope of the instep, mounting the IMU box on this area can lead to the non-parallel alignment of the pitch axes of IMU 3 and 4. Consequently, this results in a deviation between the true rotation angle of the Ankle and the angle recorded by the system. This error is systematic and can be addressed by offsetting the initial orientation of the pitch axes of IMU 4. Overall, the results affirm the potential application of the system in assessing the range of motion for patients in the future.

Conclusion

This research proposed a system to measure joint angles using IMU sensors in the application of assisting the evaluation of lower limb rehabilitation in stroke patients. Euler angles were extracted from the sensors and sent to microcontroller Arduino Mega 2560 via I2C protocol on which the calculations were done. The system commnunicated with a computer via USB connection, where the results were presented and logged. Experiments carried out consisted of doing exercises from the Fugl-Meyer Assessment while using the system proposed and VICON motion capture system, both to verify the system's effectiveness in the rehabilitation evaluation process, and to assess the accuracy of the system.

The comparison demonstrated that the system performed acceptably well in Hip Flexion and Knee Flexion exercises, but lacked precision in Ankle Dorsiflexion exercise. This deviation could be explained to be related to the shape of the foot and placement of the IMU sensor onto the dorsum of the foot. Nevertheless, this study showed the possibility of integrating IMU sensors in lower limb rehabilitation assessment, and the promise of a joint angles measuring system which is affordable, portable and suitable for a wide range of ages. Future work to improve the system developed in this paper could involve better designed boxes to provide greater fit for IMU placements, wireless data transmission for faster and more convenient usage, and a desktop application for easier recordings of angle data and patients' information.

Acknowledgement

The authors would like to express appreciation to the members of Komeda VN Laboratory, BioMechanics Research Group from SME- HUST and Orthopedic & Sports medicine Center, Vinmec Healthcare System, Vietnam for their assistance in the development of this research.

Appendix

Table 1
Details in IMU box assembly

Name	Number	Function
IMU Box cover	4	Contain and protect the IMU, clip the IMU signals wires, with waiting holes to attach the belt
Joint belt clamp	4	Attach the IMU to the joint belt
IMU	4	Collect motion data and send data to the Controller
Joint belt	4	Fix the IMU box at predetermined positions on the body to reduce the vibration of the IMU box when measuring motion data

Table 2
Details in controller box assembly

Name	Number	Function
Board Arduino Mega 2560	1	Receive signals from IMUs and send signal to computer
PCB shield	1	Intermediate connection between IMU sensors, TCA9548A and Arduino
TCA9548A	1	Expanding the I2C communication pins between the master (Arduino Mega 2560) and slaves (IMU sensors)
Jack GX16-4P	4	Connect IMU sensor signal wires to Controller Box easily, ensuring a secure and reliable connection

Controller Box cover	1	Protect the components inside the Controller box, contain and fix the position of the components inside the Controller Box, with waiting holes on the side wall to attach the jack plugs
Waist belt clamp	1	Attach to the bottom of the Controller Box, clip the belt to fix the position of the Box when the posture changes
Waist Belt	1	Fix the position of the Controller Box on the lower abdomen, limiting the shaking of the Controller Box when the user moves

References

[1] *World Stroke Day*. https://www.who.int/southeastasia/news/detail/2810-2021-world-stroke-day. Accessed: [08/12/2023]

[2] *World Stroke Organization Global Stroke Fact Sheet*. https://www. world-stroke.org/assets/downloads/WSO_Global_Stroke_Fact_Sheet.pdf. Accessed: [08/12/2023]

[3] Duy Ton Mai et al. "Current State of Stroke Care in Vietnam". In: *Stroke: Vascular and Interventional Neurology* 2.2 (2022), e000331. DOI: 10.1161/SVIN.121.000331.URL:https://www.ahajournals.org/doi/abs/10.1161/SVIN.121.000331

[4] *Vietnam Stroke Statistics*. https://www.worldlifeexpectancy.com/ viet-nam-stroke. Accessed: [08/12/2023]

[5] *Chances of Recovery from Stroke Paralysis*. https : / / www . flintrehab. com / chances - of - recovery - from - stroke - paralysis/. Accessed: [08/12/2023]

[6] Karen J. Sullivan et al. "Fugl-Meyer assessment of sensorimotor function after stroke: standardized training procedure for clinical practice and clinical trials". In: Stroke 42.2 (2011), pp. 427-432

[7] David J. Gladstone, Cynthia J. Danells, and Sandra E. Black. "The Fugl-Meyer assessment of motor recovery after stroke: a critical review of its measurement properties". In: *Neurorehabilitation and Neural Repair* 16.3 (2002), pp. 232-240

[8] Saba Bakhshi, Mohammad H. Mahoor, and Bradley S. Davidson. "Development of a body joint angle measurement system using IMU sensors". In: *2011 Annual International Conference of the IEEE Engineering in Medicine and Biology Society*. 2011, pp. 6923-6926, DOI: 10.1109/IEMBS.2011.6091743

[9] Jonathan F S Lin and Dana Kulic. "Human pose recovery using´ wireless inertial measurement units". In: *Physiological Measurement* 33.12 (Nov.

2012), p. 2099, DOI: 10.1088/0967-3334/33/ 12/2099. URL: https://dx.doi.org/10.1088/0967-3334/33/12/2099

[10] Sumit Majumder and M. Jamal Deen. “Wearable IMU-Based System for Real-Time Monitoring of Lower-Limb Joints”. In: *IEEE Sensors Journal* 21.6 (2021), pp. 8267-8275, DOI: 10.1109/ JSEN.2020.3044800

[11] Wesley Niswander, Wei Wang, and Kimberly Kontson. “Optimization of IMU Sensor Placement for the Measurement of Lower Limb Joint Kinematics”. In: *Sensors* 20.21 (2020) ISSN: 14248220. DOI: 10.3390/s20215993. URL: https://www.mdpi.com/ 1424-8220/20/21/5993

[12] Bosch Sensortec. *BNO055 Datasheet*. Datasheet. Nov. 2014. URL: https : / / www. alldatasheet . com / datasheet - pdf / pdf / 1132074 / BOSCH/BNO055.html

[13] Christopher P Walmsley et al. “Measurement of Upper Limb Range of Motion Using Wearable Sensors: A Systematic Review”. In: *Sports Med Open* 4.1 (Nov. 2018), p. 53, DOI: 10 .1186 / s40798-018-0167-7

[14] *Lower Body Modeling with Plug-in Gait*. https://docs.vicon.com/ display/Nexus212/Lower+body+modeling+with+Plug-in+Gait. Accessed: [08/12/2023]

[15] *NIHSS: Everything You Need to Know About the National Institutes of Health Stroke Scale*. https://www.neurolutions.com/aboutstroke/nihss-everything-you-need-to-know-about-the-nationalinstitutes-of-health-stroke-scale/. Accessed: [08/12/2023]

[16] *Canadian Neurological Scale (CNS)*. https : / / strokengine . ca / en / assessments / canadian - neurological - scale - cns/. Accessed: [08/12/2023]

[17] Martin Taylor-Rowan et al. “Functional Assessment for Acute Stroke Trials: Properties, Analysis, and Application”. In: *Frontiers in Neurology* 9 (2018) ISSN: 1664-2295. DOI: 10.3389/fneur. 2018.00191. URL: https://www.frontiersin.org/articles/10.3389/ fneur.2018.00191

[18] *Fugl-Meyer Assessment for Motor Recovery after Stroke*. https: //www.sralab.org/rehabilitation-measures/fugl-meyer-assessmentmotor-recovery-after-stroke. Accessed: [08/12/2023]

[19] A. R. Fugl-Meyer et al. “The post-stroke hemiplegic patient. 1. a method for evaluation of physical performance”. In: *Scandinavian journal of rehabilitation medicine* 7.1 (1975), pp. 13-31

[20] S. Majumder Deen and M. J. “Wearable IMU-Based System for Real-Time Monitoring of Lower-Limb Joints”. In: *IEEE Sensors Journal* 21.6 (2021), pp. 8267-8275, DOI: 10.1109/JSEN.2020. 3044800

[21] W. Niswander, W. Wang, and K. Kontson. “Optimization of IMU Sensor Placement for the Measurement of Lower Limb Joint Kinematics”. In:

Sensors (Basel, Switzerland) 20.21 (2020) p. 5993, DOI: https://doi.org/10.3390/s20215993

[22] Jill See et al. “A Standardized Approach to the Fugl-Meyer Assessment and Its Implications for Clinical Trials”. In: *Neurorehabilitation and Neural Repair* 27.8 (2013) PMID: 23774125, pp. 732-741, DOI: 10.1177/1545968313491000, URL: https://doi.org/10.1177/1545968313491000

[23] Rudolf Kalman. “A new approach to linear filtering and prediction”. In: *Transactions of ASME, Journal of Basic Engineering on Automatic Control* (1960), pp. 35-45

[24] Xuyou Li et al. “Temperature Dependence of Faraday EffectInduced Bias Error in a Fiber Optic Gyroscope”. In: *Sensors* 17.9 (2017) ISSN: 1424-8220, DOI: 10.3390/s17092046. URL: https: //www.mdpi.com/1424-8220/17/9/2046

[25] Shinji Mitani et al. “Analysis of temperature-induced drift rate error in interferometric multi-core fiber optic gyroscope”. In: *International Conference on Space Optics* — ICSO 2020. Ed. by Bruno Cugny, Zoran Sodnik, and Nikos Karafolas. Vol. 11852. International Society for Optics and Photonics. SPIE, 2021, 118523E. DOI: 10.1117/12.2599545. URL: https://doi.org/10. 1117/12.2599545

[26] Yunhao Zhang, Yonggang Zhang, and Zhongxing Gao. “Thermalinduced phase-shift error of a fiber-optic gyroscope due to fiber tail length asymmetry”. In: *Appl. Opt*. 56.2 (Jan. 2017), pp. 273-277, DOI: 10.1364/AO.56.000273.
URL:https://opg.optica.org/ao/abstract.cfm?URI=ao-56-2-273

[27] F. Mumuni and A. Mumuni. “Adaptive Kalman filter for MEMS IMU data fusion using enhanced covariance scaling”. In: *Control Theory Technol*. 19 (2021) pp. 365-374, DOI: 10.1007/s11768021-00058-8. URL: https://doi.org/10.1007/s11768-021-00058-8

[28] Patrick Slade et al. “An Open-Source and Wearable System for Measuring 3D Human Motion in Real-Time”. In: *IEEE Transactions on Biomedical Engineering* 69.2 (2022) pp. 678-688, DOI: 10.1109/TBME.2021.3103201